Supplement to Maier et al.: „Quantifying Retrogressive Thaw Slump Mass Wasting and Carbon Mobilisation on the Qinghai-Tibet Plateau Using Multi-Modal Remote Sensing "

Table S1: Detailed results of RTS activity between 2011 and 2020 in QTP and its subregions. We report the median quantities per RTS including entire area A_{Xia}, actively eroding area δA, median and maximum (95th percentile) elevation change (~ headwall height) δh and δh_{max}, and volume change of thawed material δv, as well as the total estimates as the sum over all RTS per region including volume change of thawed material δV (lower and upper bounds $\delta V^{-/+}$).

		Per RTS					Total		
	n	A_{Xia}	δA	δh	δh_{max}	δV	δV	δV^-	δV^+
Region		[10^3 m^2]		[m]		[10^3 m^3]	[10^6 m^3]		
West	170	4.45	2.75	1.65	4.80	5.74	1.60	0.10	12.09
West-Central	523	6.80	4.20	1.01	2.04	4.73	4.14	0.31	39.55
Central	2688	8.70	5.80	1.22	2.32	6.89	39.28	5.56	178.52
East	76	4.55	2.90	0.84	1.85	2.48	0.40	0.05	3.50
Northeast	140	9.15	5.50	2.21	4.99	12.90	4.29	1.43	16.47
QTP	**3613**	**8.00**	**5.20**	**1.21**	**2.54**	**6.33**	**50.24**	**7.46**	**253.49**

Table S2: Detailed results of RTS induced ground ice loss and OC mobilisation between 2011 and 2020 in QTP and its subregions. We report total ground ice loss δGI and its lower and upper bounds $\delta GI^{-/+}$, the total amount of SOC that has been mobilized due to RTS activity δOC including lower and upper bounds $\delta OC^{-/+}$, as well as the OC fluxes δOC_{flux} (lower and upper bounds $\delta OC_{flux}^{-/+}$) that represent δOC normalized by the number of years of the temporal baseline of the DEM.

	δGI	δGI^-	δGI^+	δOC	δOC^-	δOC^+	δOC_{flux}	δOC_{flux}^-	δOC_{flux}^+
Region		[10^5 m^3]			[10^7 kg C]			[10^6 kg C a^{-1}]	
West	0.64	0.04	6.15	0.35	0.00	1.70	0.42	0.00	2.09
West-Central	1.96	0.12	32.28	1.76	0.00	7.35	2.27	0.00	9.43
Central	31.94	2.29	232.85	22.63	0.41	62.57	28.58	0.52	79.13
East	0.19	<0.01	4.37	0.54	<0.01	1.87	0.67	<0.01	2.31
Northeast	1.05	0.32	4.26	2.26	0.69	5.27	3.05	0.95	7.04
QTP	**35.81**	**2.80**	**281.99**	**27.83**	**1.11**	**79.80**	**35.34**	**1.47**	**101.28**

Table S3: Validation of the planimetric area and material erosion volume estimated based on RTS delineations of Xia et al. (2024) from summer 2018, 2019, and 2020 and the elevation change between TanDEM-X DEM from winter 2011 and 2019. We report the estimated actively eroding area estimated from the inventory overlapping only negative elevation change δA for 2018. 2019 and 2020 as well as the volume change of the eroded material δV (including the propagated height error σ_v). The validation δA and δV values come from a manual delineation of the negative elevation change for 307 RTS in five test sites distributed across the subregions in QTP.

Test site	δA [10^5 m^2] val.	2018	2019	2020	δV ± σ_V [10^5 m^3] val.	2018	2019	2020
A Western Kunlun	2.20	4.75	5.00	5.37	9.19 ± 1.59	10.42 ± 3.97	11.01 ± 4.19	11.83 ± 4.43
B Gaize	0.23	0.22	0.25	0.27	0.44 ± 0.13	0.38 ± 0.15	0.43 ± 0.16	0.46 ± 0.16
C Southern Nima	2.14	2.18	2.30	2.39	3.70 ± 0.40	3.30 ± 0.40	3.46 ± 0.41	3.57 ± 0.42
D Beiluhe River Basin	36.04	33.74	41.80	49.20	78.58 ± 8.10	62.58 ± 8.46	76.09 ± 9.77	84.65 ± 10.52
E Qilian Mountain	1.68	2.84	3.31	3.54	7.48 ± 1.63	7.99 ± 2.58	8.83 ± 3.04	9.19 ± 3.08
All test sites	**42.28**	**43.72**	**52.65**	**60.77**	**99.39 ± 11.84**	**84.66 ± 15.55**	**99.81 ± 17.56**	**109.69 ± 18.61**

Table S4: Comparison between VHR DEM based on drone photogrammetric survey in summer 2020 at 6 RTS in the Beiluhe River Basin in central QTP and the elevation change computed from the boundaries of the optical RTS inventory (Xia et al. 2024) and the TanDEM-X DEM (2011-2019). The median headwall height is a direct measurement differences of elevations from stable terrain above the headwall and elevations from the slump floor close to the headwall in the VHR DEM and indirectly computed for the TanDEM-X elevation change by dividing the volume change of the eroded material δV by the erosion affected area δA. The maximum elevation change within the actively eroding area of the RTS gives an indication of the potential headwall height and is used for the comparison to the VHR DEM. For all values, we report the standard deviation / error estimate σ.

RTS	Location	Initiation	RTS area Total [m^2]	Active [%]	VHR $\bar{h}$ [m]	TanDEM-X δh_{max} [m]
1	34.647° N, 92.936° E	2017	7265	77	2.76 ± 1.19	3.04 ± 1.91
2	34.731° N, 92.871° E	2017	9141	78	3.08 ± 1.06	3.78 ± 2.57
3	34.710° N, 92.887° E	2017	2536	81	1.10 ± 0.83	2.93 ± 1.85
4	34.708° N, 92.883° E	2017	9637	53	3.55 ± 0.75	3.83 ± 2.78
5	34.647° N, 92.928° E	2019	3891	69	1.99 ± 1.99	3.32 ± 2.46
6	34.646° N, 92.926° E	2019	1087	100	1.89 ± 0.98	1.83 ± 1.56

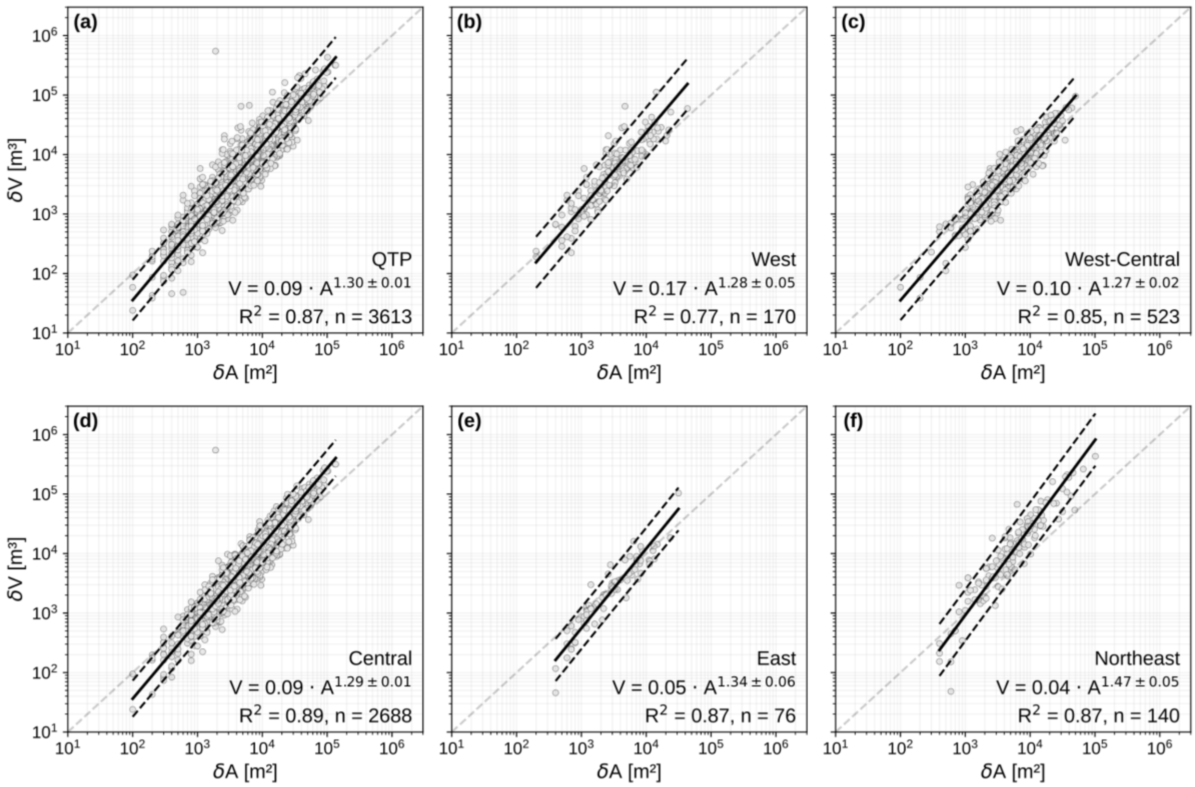

Figure S1: Allometric scaling between the actively eroding area of the delineated scar zone δA of the optical RTS inventory and the computed volume change based on the elevation change of the TanDEM-X DEM (T2-T1) within the actively eroding area. **(a)** For the entire QTP with n_{RTS} = 3613, we found a scaling coefficient α = 1.30 $\pm$ 0.01 with R^2 = 0.87. **(b) – (f)** For the QTP subregions, we found α-values between 1.27 and 1.47 with R^2-values between 0.77 and 0.89.

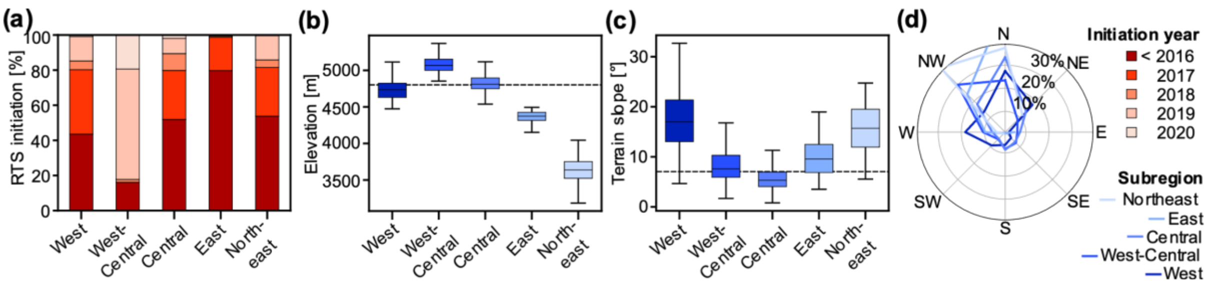

Figure S2: Temporal and terrain characteristics of RTS present in the optical inventory of Xia et al. (2024) in the subregions of QTP. **(a)** Percentage of RTS per initiation year. **(b)** Distribution of elevation of the RTS location. **(c)** Distribution of the slope of the average terrain at the RTS location. **(d)** Main terrain aspect of RTS.

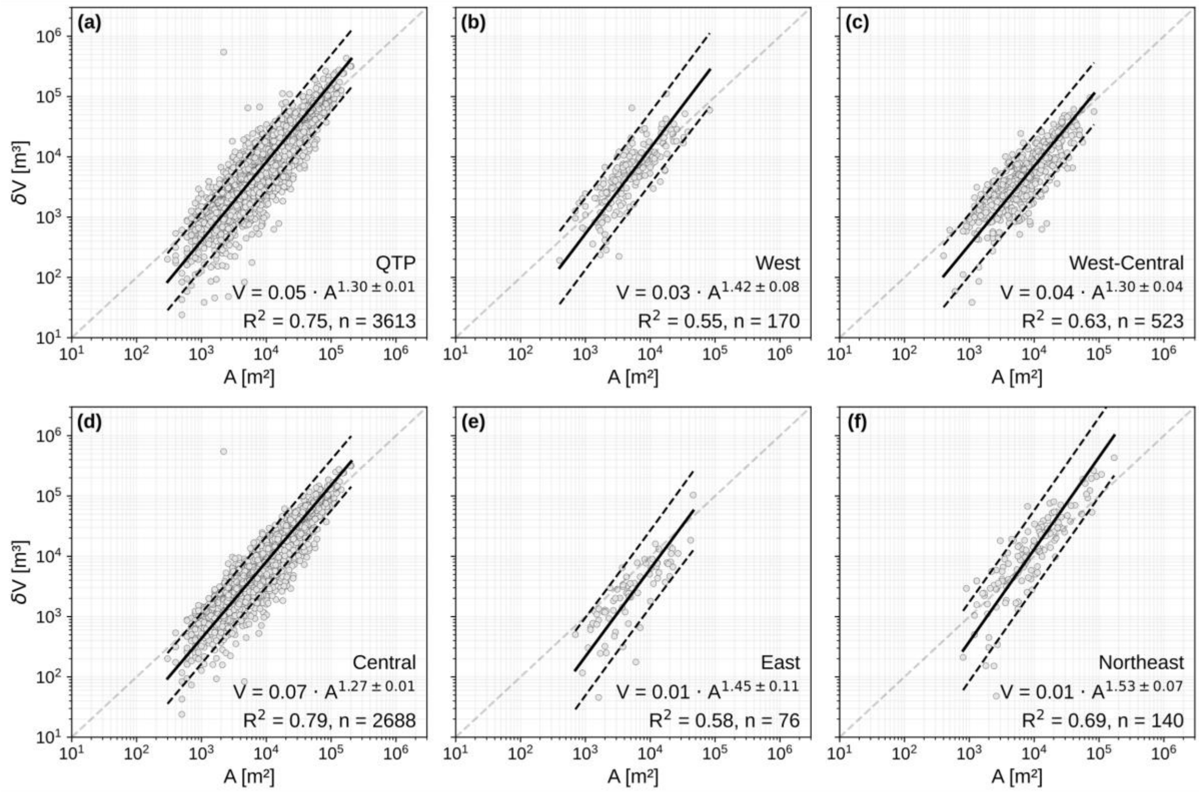

Figure S3: Allometric scaling between the entire area of the delineated scar zone A_{Xia} of the optical RTS inventory and the computed volume change based on the elevation change of the TanDEM-X DEM (T2-T1) within the actively eroding area. **(a)** For the entire QTP with n_{RTS} = 3613, we found a scaling coefficient α = 1.30 $\pm$ 0.01 with R^2 = 0.75. **(b) – (f)** For the QTP subregions, we found α-values between 1.27 and 1.30 in the QTP's central regions and higher α-values between 1.42 and 1.53 in the west, east and northeast of the plateau with subregion R^2-values between 0.55 in the West and 0.79 in Central QTP.